EURASIAN PHYSICAL TECHNICAL JOURNAL

2024, Volume 21, No. 3 (49)

https://doi.org/10.31489/2024No3/29-36

Received: 11/06/2024 Revised: 27/08/2024 Accepted: 13/09/2024 Published online: 30/09/2024

Research Article

UDC: 537.622.3:620.193.4:699.15

CORROSION BEHAVIOUR OF MAGNESIUM ALLOYS NZ30K AND NZ30K ALLOYED WITH SILVER IN THE MODEL SOLUTION OF THE OSTEOSYNTHESIS PROCESS

Greshta V.[1], Narivskyi O.[1,2], Dzhus A.[1], Vynar V.[3], Yar-Mukhamedova G.[4], Mukashev K.[5], Beissen N.[4], Mussabek G.[4], Imanbayeva A.[4,6*], Zelele D.[4], Atchibayev R.[4], Kemelzhanova A.[4]

[1] National University "Zaporizhzhya Polytechnic", Ukraine
[2] Ukrspetsmash LLC, Berdiansk, Ukraine
[3] Karpenko Institute of Physics and Mechanics of the National Academy of Sciences of Ukraine, Lviv, Ukraine
[4] Al-Farabi Kazakh National University, Almaty, Kazakhstan
[5] Energo University, Almaty, Kazakhstan
[6] Research Centre "KazAlfaTech LTD", Almaty, Kazakhstan
*Corresponding author: akmaral@physics.kz

Abstract. *The corrosion behaviour of magnesium alloys NZ30K and NZ30K alloyed with 0.1 wt.% silver in Ringer's Locke solution has been studied, since their components are not toxic to the human body and do not cause clinical complications in the treatment of bone fractures, and silver has antibacterial properties inherent in antibiotics. It has been found that the E_{cor} potential of the silver-alloyed NZ30K sample was -1.57V during the first 100 seconds of testing, but then it intensively shifted to the positive side to -1.54V within 512 seconds at a rate of 0.051 mV/s, which decreased to 0.014 mV/s after the next 1000 seconds, and a stationary value of the potential E_{cor} on the sample has been recorded. The sample to uniform general corrosion has been subjected, and the improvement of its potential E_{cor} during its corrosion study was due to the most intense selective dissolution of magnesium, which has the most negative value of the standard potential among the alloy components, and the enrichment of its surface with Zn, Nd, Zr, Ag, which have a positive value of the standard potential. This trend contributed to a decrease in the rate of general corrosion and made it impossible to develop local corrosion. The NZ30K alloy alloyed with 0.1 wt.% silver is recommended for further potentiodynamic and volumetric corrosion studies to justify its selection as a structural material for the production of biodegradable implants in osteosynthesis.*

Keywords: bioimplant, magnesium alloy NZ30K alloyed with silver, local corrosion, osteosynthesis

1. Introduction

The controlled corrosion behaviour of magnesium alloys supports the development of advanced biodegradable implants for surgical treatment in traumatology [1]. Magnesium is a very reactive metal and corrodes rapidly in body fluids because it is unable to form self-protective oxide films [2]. Magnesium alloys in the state of supply have low mechanical characteristics, which makes it impossible to produce biodegradable implants for surgery. Currently, two approaches are used to improve the mechanical, physical, chemical, and biological properties of magnesium implants, including various methods of magnesium alloying [3-5] and grinding the microstructure to ultrafine or nanoscale grain [6-8].

Al, Ca, Cu, Fe, Li, Mn, Ni, Sr, Y, Zn, Zr are most commonly used to alloy Mg, and rare earth elements are used to modify its structure [9,10]. Aluminium-containing alloys are most commonly used in the production of biodegradable implants because they have excellent casting properties, high strength, and good relative elongation [11]. However, the corrosion products of this alloy contain AlO_{23} oxide, which can contribute to Alzheimer's disease, muscle breakdown, and reduced osteosynthesis [12]. The magnesium alloy NZ30K, unlike Al-containing alloys based on Al-Ca, Al-Zn, and Al-Li [13], does not have such disadvantages. In addition, the mechanical properties of NZ30K magnesium alloy have high performance for the production of biodegradable implants, since their yield strength (140 MPa) [14] is higher than that of tubular bones (120 MPa) [15]. At the same time, the alloying of NZ30K alloy with silver in the amount of 0.1 wt. % increased its temporary tensile strength (σ_B) by 8.6 and relative elongation by 63.9% [16]. In addition, it has antibacterial properties characteristic of antibiotics [17], but long-term (6 weeks) corrosion tests of samples in a solution of helofusin (an artificial blood substitute) contributed to its reduction by 22.9% [16]. At the same time, after prolonged corrosion tests of the alloy, this figure was 205 MPa [16], which is significantly higher than the strength of tubular bones [15], and the presence of silver in the alloy gives it antibacterial properties [17]. If the corrosion test results of silver-alloyed NZ30K alloy are satisfactory, it can be recommended for the manufacture of biodegradable implants and clinical testing. Therefore, we studied the corrosion behaviour of this alloy in Ringer-Locke solution.

2. Research materials and methods

We studied samples of magnesium alloys NZ30K and NZ30K alloyed with silver in the amount of 0.1 wt.% smelted in an induction crucible furnace and subjected to aging [16]. The diameter of the samples was 12 and the length was 30 mm. Their chemical composition by the X-ray spectral method at the installation INKA ENERGY 350 has been determined (Table 1).

Table 1. Chemical composition of the studied samples.

Alloy	Content of chemical elements, wt. %				
	Mg	Zn	Zr	Nd	Ag
NZ30K	95.67	0.67	0.89	2.77	-
NZ30K + Ag	95.57	0.69	0.86	2.79	0.09

Corrosion tests of the samples in a Ringer-Locke solution (an aqueous solution of bi-distilled water with the following chemicals, in mg/l: NaCl – 9; $NaHCO_3$; $CaCl_2$; KCl по 0,2; $C_6H_{12}O_6$ – 1) at a temperature of 20±1°C has been carried out. The establishment of a stationary value of the corrosion potential E_{cor} on the tested samples on the PN-2MK-10A potentiostat in automatic mode has been recorded. The surface of corrosion damage on the samples after their testing in Ringer Locke's solution using an optical microscope MMR-2P has been examined.

3. Research results and discussion

According to the results of the corrosion test of the NZ30K alloy sample (Table 1) in a Ringer-Locke solution at 20°C, it has been found that its corrosion potential E_{cor} slowly shifted to the positive side from -1.579 to -1.576V during 1400 seconds of testing (Fig. 1, curve 1). Thus, the rate of this process was 0.0021 mV/s. Most likely, this trend is due to the formation of a magnesium hydroxide precipitate coating on the alloy surface. After 1400 seconds of exposure of the sample to the test solution, a shift of the potential E_{cor} in the negative direction by about 2 mV within 100 seconds and a shift of its value in the opposite direction with the same intensity have been observed. After that, during 200 seconds of testing, the steady-state value of this potential at -1.575 V has been recorded (Fig. 1, curve 1). The characteristic small fluctuation of the potential E_{cor} during the establishment of its steady-state value is most likely due to the delamination of the magnesium hydroxide precipitate coating on the surface of the sample in the vicinity of corrosion ulcers and other corrosion damage formed near intermetallic compounds, which were identified in [16]. This is consistent with the data from [18-20] on the nucleation and growth of pitting in the vicinity of inclusions in passivated steels and alloys.

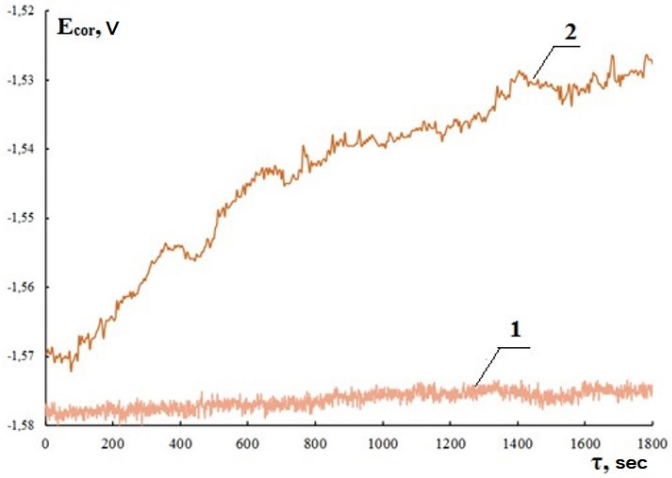

Fig.1. Dependence between the corrosion potential E_{cor} of NZ30K alloy (1) and NZ30K alloy alloyed with 0.1 wt. % silver (2) on the time of corrosion tests (τ) of the sample in Ringer-Locke solution at a temperature of 20° C.

It has been found that the sample subjected the greatest corrosion damage in the peripheral areas, i.e., in the places of the greatest plastic deformation of the alloy and the number of microdefects on its surface associated with the casting technology (Fig. 2, a).

a) *b)*

Fig.2. Corrosion damage on the end surface of NZ30K alloy (a) and silver alloyed NZ30K (b) samples after corrosion tests in Ringer-Locke solution.

These places are most often the focus of the origin and growth of local corrosion damage in chloride-containing media, such as Ringer-Locke solution. In particular, it has been found that the area of local corrosion damage on the end surface of the cylindrical specimen was 8.78 mm^2, which is 17.5% of the area of the end surface of the cylindrical specimen (Table 2).

Table 2. Area of corrosion damage on the end surfaces of the tested samples

No.	Sample	Corrosion damage area, mm^2	% of the end surface area of the sample
1	NZ30K alloy	8.78	17.5
2	NZ30K alloy additionally alloyed with Ag	8.12	16.24

Note: total end surface area of the sample is 50.24 mm^2.

About 90% of the local corrosion damage at the intersection of the cylindrical and flat surfaces of the sample has been recorded. In general, its cylindrical surface to intense local corrosion in the form of pitting and deep corrosion ulcers has been subjected (Fig. 3, a). This type of corrosion damage is typical for passivated steels and alloys in chloride-containing media [20]. Zirconium and zinc contribute to the formation of a dense oxide film on the surface of the magnesium alloy NZ30K, which can be locally damaged by chloride ions in the vicinity of intermetallic inclusions found in the alloy [16]. Such areas on the surface of steels and alloys are the most likely centres of pitting nucleation and growth observed on the surface of the NZ30K alloy sample (Fig. 3, a). Summarizing the above, it can be noted that NZ30K alloy under intensive pitting in a Ringer-Locke solution with active hydrogen release, so it cannot be used for the production of biodegradable implants without improving its resistance to local corrosion. Alloying NZ30K alloy with silver in the amount of 0.1 wt.% significantly changed its corrosion behaviour.

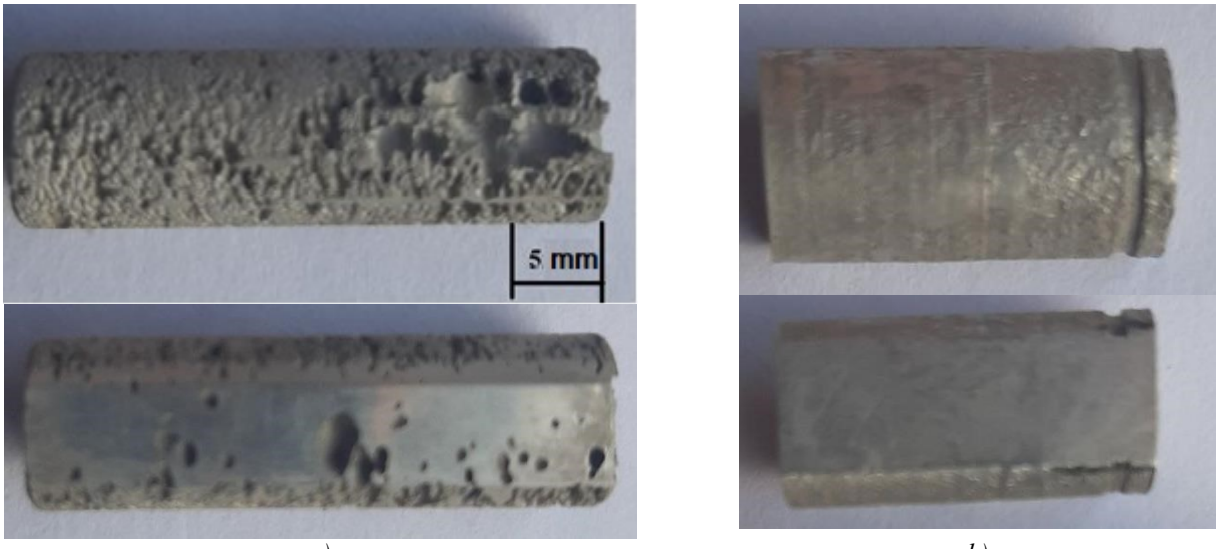

a) *b)*

Fig.3. Corrosion damage on the cylindrical surface of NZ30K alloy (a) and silver-alloyed NZ30K (b) samples after corrosion tests in Ringer-Locke solution.

In particular, according to the results of a corrosion study of a sample made of NZ30K alloy alloyed with Ag in Ringer-Locke solution, it has been found that its corrosion potential E_{cor} after immersion in the solution was ~ -1.57 V (Fig. 1, curve 2) and remained practically unchanged for 100 seconds (points 1-4 of Table 3).

However, in the interval from 100 to 612 seconds of testing, it shifted intensively to the positive side to -1.54432 V (point 20 of Table 3). Thus, it turns out that the rate of shift of the potential E_{cor} in the positive direction was 0.051 mV/s. Then, in the interval from 612 to 1620 seconds, it decreased to 0.014 mV/s, and from 1620 to 1800 seconds of testing, the sample recorded a stationary value of the potential E_{cor} ~ -1.52 V. It turns out that the steady-state value of the potential E_{cor} of the NZ30K alloy alloyed with Ag was set from -1.5696 (point 1) to -1.52716 V (point 40 of Table 3) within 1800 seconds.

The characteristic features of establishing the stationary value of the potential E_{cor} of the NZ30K alloy alloyed with Ag in Ringer-Locke solution are due to the different intensity of dissolution of its components, which formed the microrelief of the sample surface after its corrosion test (Fig. 2, b). In (Fig. 2, b), we observed etched areas of metal in the form of irregularly shaped black spots up to 500 μm in size, which is characteristic of corrosion destruction of micro volumes of metal in the vicinity of inclusions at the intersection with alloy grain boundaries [20, 21] and multidirectional curved lines, which is inherent in the local selective dissolution of metals by grain boundaries in alloys and steels. It should be noted that the area of corrosion damage on the end surfaces of the silver-alloyed NZ30K sample is 7.8% smaller than that of the MZ30K sample (Table 2). It is obvious that secondary phases, grain size, and structure affect the corrosion rate [22, 23]. In particular, works [24, 25] found that the larger the mean austenite grain diameter of the studied steels and alloys, the less likely they are to intersect with inclusions in the vicinity of which pitting occurs and develops, which under certain conditions can turn into corrosion ulcers.

Table 3. Corrosion potentials E_{cor} of NZ30K alloy alloyed with Ag depending on the sample holding time (τ) in Ringer-Locke solution

No. of points	τ, s	E_{cor} , V	No. of points	τ, s	E_{cor} , V
1	4	-1.5696	21	852	-1.53792
2	36	-1.57024	22	884	-1.53952
3	68	-1.57024	23	948	-1.5392
4	100	-1.56704	24	980	-1.53888
5	132	-1.56896	25	1012	-1.53888
6	164	-1.56448	26	1044	-1.53824
7	196	-1.56416	27	1108	-1.53696
8	228	-1.56224	28	1140	-1.53664
9	260	-1.56064	29	1204	-1.53664
10	292	-1.55872	30	1236	-1.53664
11	324	-1.55648	31	1300	-1.53536
12	356	-1.5536	32	1332	-1.5344
13	388	-1.55424	33	1364	-1.5328
14	420	-1.55488	34	1492	-1.53088
15	452	-1.55552	35	1556	-1.53184
16	484	-1.55328	36	1588	-1.5312
17	516	-1.54976	37	1620	-1.53024
18	548	-1.54816	38	1716	-1.52928
19	580	-1.54688	39	1748	-1.52864
20	612	-1.54432	40	1800	-1.52768

Secondary phases, inclusions, and grain size of Ag alloy NZ30K alloy alloyed with Ag are primarily caused by magnesium alloying with zinc, zirconium, neodymium, and silver (Table 1). Due to their low solubility in Mg, the metastable supersaturated solid solution can decompose naturally, forming fine inclusions in magnesium grains. They can block the increase in grain size [26]. In particular, work [16] found that alloying NZ30K alloy with silver in the amount of 0.1 wt.% contributed to a 4-fold reduction in the mean grain diameter. This may contribute to reduce the rate of general corrosion, but increase the likelihood of pitting in chloride-containing media [27]. It is also known [28], that alloying elements of magnesium alloys can create a micro-galvanic effect between the Mg matrix and various inclusions and secondary phases. They play the role of cathodes, in the vicinity of which a solid magnesium solution selectively dissolves [29]. In particular, the formation of pitting in the vicinity of the secondary phases AlMg, AlMgFe, Mg_{17} Al_{12} or Mg_2 Cu in [30] has been observed. This is consistent with the data of [18-20, 24, 25, 31] for chromium-nickel steels and alloys.

It should be noted that the sample from the NZ30K alloy of alloyed Ag 612 s after its immersion in the test solution had a potential E_{cor} =-1.544V (point 20 of Table 3), which corresponds to a change in the intensity of selective dissolution of metals from the sample surface and its enrichment with silver (the place of a rapid change in the potential E_{cor} Fig. 1, curve 2). This may be one of the reasons for the rapid, almost 5-fold decrease in the rate of shift of its potential E_{cor} to the positive side. After 1620 s of studying the alloy in the Ringer-Locke solution, the sample reached a stationary value of the potential E_{cor} =-1.53 V (point 37 of Table 3), which most likely corresponds to the process of maximum saturation of the sample surface with silver and the formation of a stable double electric layer on it.

Summarizing the above, it can be noted that the NZ30K alloy alloyed with silver in the amount of 0.1 wt.% was subjected mainly to general corrosion (Fig. 3, b), because no local corrosion damage was found on the sample cylindrical surface, which is typical for the NZ30K alloy sample (Fig. 3, a). Therefore, it is promising for the production of biodegradable implants, provided that the results of electrochemical, volumetric, and clinical studies are positive.

4. Conclusions

According to the results of corrosion studies, it has been found that the steady-state value of the corrosion potential E_{cor} of the NZ30K alloy sample has been formed from 1.579 to -1.575V during 1800 seconds of testing in the Ringer-Locke solution, and its surface to intense pitting and ulcer corrosion has been subjected with intense hydrogen release at the cathodic areas of the sample. The most intense hydrogen emission on the surface of the sample after its immersion in the test solution at the most negative value of E_{cor} has been visually recorded. It has been found that E_{cor} of the sample made of NZ30K alloy alloyed with 0.1 wt.% silver during the first 100 seconds in the solution was ~ 1.57V, then during 500 seconds of testing it shifted to the positive side at a rate of 0.051 mV/s, but in the test interval from 612 to 1620 seconds it decreased to 0.014 mV/s, and after 1800 seconds a stationary value of this potential at ~ -1.53V has been established. The sample was mainly subjected to uniform general corrosion with varying intensity until the steady-state value of E_{cor} has been established, and its ennoblement was most likely due to the most intense selective dissolution of Mg from the sample surface and its enrichment with silver, zirconium, and neodymium. This alloy is recommended for further research as a structural material for the production of biodegradable implants.

Conflict of interest statement

The authors declare that they have no conflict of interest in relation to this research, whether financial, personal, authorship or otherwise, that could affect the research and its results presented in this paper.

CRediT author statement:

Greshta V., Narivskyi O., Dzhus A, and Vynar V.: Conceptualization, Validation, and Formal analysis; Yar-Mukhamedova G., Mukashev K., Mussabek G., Zelele D., and Atchibayev R.: Validation and Investigation; Beissen N., Imanbayeva A., and Kemelzhanova A.: Verification.

The final manuscript was read and approved by all authors.

Acknowledgements

This research has been funded by the Science Committee of Kazakhstan's Ministry of Science and Higher Education (AP23484310).

References

1 Li H., Zheng Y., Qin L. (2014) Progress of biodegradable metals. *Progress in Natural Science: Materials International,* 24 (5), 414 – 422. DOI: 10.1016/j.pnsc.2014.08.014.

2 Samal S. (2016) High-Temperature Oxidation of Metals. In book: High Temperature Corrosion. 156. DOI:10.5772/63000.

3 Zeng R.-C., Sun L., Zheng Y.F., Cui H.-Z., Han E.-H. (2014) Corrosion and characterization of dual phase Mg–Li–Ca alloy in Hank's solution: The influence of microstructural features. *Corrosion Science*, 79, 69 – 82. DOI:10.1016/j.corsci.2013.10.028.

4 Cui L.Y., Li X.-T., Zeng R., Ii S., Han E.-H., Song L. (2017) In vitro corrosion of Mg–Ca alloy — The influence of glucose content. *Frontiers of Materials Science***,** 11, 284-295. DOI: 10.1007/s11706-017-0391-y.

5 Zheng Y.F., Cu X.N., Witte F. (2014) Biodegradable metals. *Materials Science and Engineering: R: Reports*, 77, 1-34. DOI: 10.1016/j.mser.2014.03.001.

6 Lowe T.C., Valiev R.Z. (2014) Frontiers for bulk nanostructured metals in biomedical applications. *Advanced Biomaterials and Biodevices*, 1 - 52. Wiley Blackwell. DOI: 10.1002/9781118774052.ch1.

7 Xu W., Birbilis N., Sha G., Wang Y., Daniels J.E., Xiao Y., Ferry M. (2015). A high-specific-strength and corrosion-resistant magnesium alloy. *Nature Materials,* 14, 1229–1235. DOI: 10.1038/nmat4435.

8 Rad H.R.B., Idris M.H., Kadir M.R. A., Farahany S. (2012) Microstructure analysis and corrosion behavior of biodegradable Mg–Ca implant alloys. *Materials & Design*, 33, 88-97. DOI: 10.1016/j.matdes.2011.06.057.

9 Müller W.D., Nascimento M.L., Zeddies M., Córsico M., Gassa L.M., Mele M.A.F.L.D. (2007). Magnesium and its alloys as degradable biomaterials: Corrosion studies using potentiodynamic and EIS electrochemical techniques. *Materials Research*, 10, 5-10. DOI: 10.1590/S1516-14392007000100003.

10 Witte F., Ulrich H., Rudert M., Willbold E. (2007) Biodegradable magnesium scaffolds: Part 1: Appropriate inflammatory response. *Journal of Biomedical Materials Research Part A*, 81, 748–756. DOI: 10.1002/jbm.a.31170.

11 Witte F., Hort N., Vogt C., Cohen S., Kainer K.U., Willumeit R., Feyerabend F. (2008) Degradable biomaterials based on magnesium corrosion. *Current Opinion in Solid State and Materials Science*, 12, 63–72. DOI:10.1016/j.cossms.2009.04.001.

12 Ferreira P.C., Piai K.D.A., Takayanagui A.M.M., Segura-Muñoz S.I. (2008) Aluminum as a risk factor for Alzheimer's disease. *Revista Latino-Americana de Enfermagem*, 16, 151-157. DOI: 10.1590/S0104-11692008000100023.

13 Bach F.W., Schaper M., Jaschik C. (2003) Influence of lithium on hcp magnesium alloys. *Materials Science Forum*, 419-422, 1037-1042. DOI: 10.4028/www.scientific.net/MSF.419-422.1037.

14 Avedesian M., Baker H. (1999) *ASM specialty handbook: Magnesium and magnesium alloys*. Materials Park, OH: ASM Intern., 327. https://s2.iran-mavad.com/book/en/asm-specialty-handbook-magnesium-and-magnesium-alloys.pdf.

15 An Y., Draughn R.A., Bonucci E. (1999) *Mechanical testing of bone and the bone-implant interface*. CRC Press, 648. DOI: 10.1201/9781420073560.

16 Greshta V., Shalomeev V., Dzhus A., Mityaev O. (2023) Study of the influence of silver alloying on the microstructure and properties of magnesium alloy NZ30K for implants in osteosynthesis. *New Materials and Technologies in Metallurgy and Mechanical Engineering*, 2, 14-19. DOI: 10.15588/1607-6885-2023-2-2. [in Ukrainian]

17 Kulyk M.F., Zasukha T.V., Lutsyuk M.B. (2012) *Saponite and aerosil in animal husbandry and medicine*. Textbook Vinnytsia, Ukraine: FOP Rogalska I.O., 362. [in Ukrainian].

18 Narivs'kyi O.E. (2005) Corrosion Fracture of Platelike Heat Exchangers. *Mater Sci*., 41, 122–128. DOI:10.1007/s11003-005-0140-8.

19 Narivs'kyi O.E. (2007) The influence of heterogeneity steel AISI321 on its pitting resistance in chloride-containing media. *Materials Science*, 2(43), 256-264. DOI: 10.1007/s11003-007-0029-9.

20 Narivs'kyi O.E. (2007) Micromechanism of corrosion fracture of the plates of heat exchangers. *Mater Sci*., 43, 124–132. DOI: 10.1007/s11003-007-0014-3.

21 Wang H., Estrin Y., Zúberová Z. (2008) Biocorrosion of a magnesium alloy with different processing histories. *Materials Letters*, 62(16), 2476-2479. DOI: 10.1016/j.matlet.2007.12.052.

22 Salahshoor M., Guo Y. (2012) Biodegradable orthopedic magnesium-calcium (MgCa) alloys, processing, and corrosion performance. *Materials (Basel)*, 5(1), 135–155. DOI: 10.3390/ma5010135.

23 Pu Z., Song G.-L., & Yang, S. (2012). Grain refined and basal textured surface produced by burnishing for improved corrosion performance of AZ31B Mg alloy. *Corrosion Science*, 57, 192-201. DOI:10.1016/j.corsci.2011.12.018.

24 Narivs'kyi O., Atchibayev R., Kemelzhanova A., Yar-Mukhamedova G., Snizhnoi G., Subbotin S., Beisebayeva A. (2022) Mathematical modeling of the corrosion behavior of austenitic steels in chloride-containing media during the operation of plate-like heat exchangers. *Eurasian Chemico-Technological Journal*, 24(4), 295-302. DOI:10.18321/ectj1473.

25 Narivskyi O.E., Subbotin S.A., Pulina T.V., Khoma M.S. (2022) Assessment and prediction of the pitting resistance of plate-like heat exchangers made of AISI304 steel and operating in circulating waters. *Materials Science*, 58, 41–46. DOI: 10.1007/s11003-022-00628-4.

26 Wang H., Estrin Y., Fu H. F. (2007) The effect of pre-processing and grain structure on the biocorrosion and fatigue resistance of magnesium alloy AZ31. *Advanced Engineering Materials*, 9(11), 967-972. DOI:10.1002/adem.200700200.

27 Südholz A.D., Kirkland N.T., Buchheit R.G., Birbilis N. (2010) Electrochemical properties of intermetallic phases and common impurity elements in magnesium alloys. *Electrochemical and Solid-State Letters*, 14(2), C5. DOI:10.1149/1.3523229.

28 Zeng R.-C., Zhang J., Huang W.-J., Dietzel W., Kainer K.U., Blawert C., Wei K.E. (2006) Review of studies on corrosion of magnesium alloys. *Transactions of Nonferrous Metals Society of China*, 16(2), 763-771. DOI:10.1016/S1003-6326(06)60297-5.

29 Kozlovskiy A. (2024) Study of the influence of the accumulated dose of damage in the near-surface layer on resistance to external influences associated with corrosion processes during high-temperature annealing. *Eurasian Physical Technical Journal*, 21(1(47)), 14–20. DOI: 10.31489/2024No1/14-20.

30 Ghali E. (2010) Properties, use, and performance of magnesium and its alloys in *Corrosion resistance of aluminum and magnesium alloys: Understanding, performance, and testing.* Wiley. Parts 3. 319 – 347. DOI:10.1002/9780470531778.ch9.

31 Narivskyi O.E., Belikov S.B., Subbotin S.A., Pulina T.V. (2021) Influence of chloride-containing media on the pitting resistance of AISI321 steel. *Materials Science*, 57(2), 291-297. DOI:10.1007/s11003-021-00544-z.

AUTHORS' INFORMATION

Greshta, Victor Leonidovich – Candidate of Technical Science, Professor, National University «Zaporizhzhia Polytechnic»: Zaporizhzhia, Ukraine; Scopus Author ID: 55944039900; ORCID ID: 0000-0002-4589-6811; greshtaviktor@gmail.com

Narivskyi, Oleksii Eduardovich – Doctor of Technical Sciences, Professor, National University "Zaporizhzhya Polytechnic", Ukraine; Ukrspetsmash LLC, Berdiansk, Ukraine; Scopus Author ID: 22035375800; ORCID ID: 0000-0003-2934-183X; amz309@ukr.net
Dzhus, Anna Vyacheslavivna – PhD Student, Senior Lecturer, National University "Zaporizhzhya Polytechnic", Ukraine; Scopus Author ID: 58722586900; ORCID ID: 0000-0002-6474-0732; anna-92@ukr.net
Vynar, Vasyl Andriyovich - Doctor of Technical Science, Senior Researcher, Karpenko Institute of Physics and Mechanics of the National Academy of Sciences of Ukraine, Lviv, Ukraine; Scopus Author ID: 8630747800; ORCID ID: 0000-0002-5314-7052; vynar.va@gmail.com
Yar-Mukhamedova, Gulmira Sharipovna – Doctor of Phys. and Math. Sciences, Professor, Al-Farabi Kazakh National University, Almaty, Kazakhstan; Scopus Author ID: 6505954975; ORCID ID: 0000-0001-5642-3481; gulmira-alma-ata@mail.ru
Mukashev, Kanat – Doctor of Phys. and Math. Sciences, Professor, Energo University, Almaty, Kazakhstan; Scopus Author ID: 10640069200; ORCID ID: 0000-0002-3568-7143; mukashev.kms@gmail.com
Beissen, Nurzada Abdibekovna – Candidate of Phys. and Math. Sciences, Associate Professor, Al-Farabi Kazakh National University, Almaty, Kazakhstan; Scopus Author ID: 26530753300; ORCID ID: 0000-0002-1957-2768; nurabd@mail.ru
Mussabek, Gauhar Kalizhanovna – PhD (Sci.), Associate Professor, Al-Farabi Kazakh National University, Almaty, Kazakhstan; Scopus Author ID: 37028867500; ORCID ID: 0000-0002-1177-1244; gauhar-mussabek@mail.ru
Imanbayeva, Akmaral Karimovna – Candidate of Phys. and Math. Sciences, Researcher, Al-Farabi Kazakh National University; KazAlfaTech LTD", Almaty, Kazakhstan; Scopus Author ID: 15054326000; ORCID ID: https://orcid.org/0000-0001-9900-9782; akmaral@physics.kz
Zelele, Daniel – PhD student, Al-Farabi Kazakh National University, Almaty, Kazakhstan**;** ORCID ID: 0009-0003-1085-5264; danielmekonnenz@gmail.com
Atchibayev, Rustem Alibekovich – PhD, Al-Farabi Kazakh National University, Almaty, Kazakhstan; Scopus Author ID: 57202802182; ORCID ID: 0000-0002-1959-7199; rustematch@gmail.com
Kemelzhanova, Aiman Esteuovna – Master (Eng.), Al-Farabi Kazakh National University, Almaty, Kazakhstan; Scopus Author ID: 57216317480; ORCID ID: 0000-0002-3406-9714; aiman_90.08@mail.ru